Hindawi
Shock and Vibration
Volume 2019, Article ID 8253269, 14 pages
https://doi.org/10.1155/2019/8253269

Research Article

Mechanism by Which Backfill Body Reduces Amount of Energy Released in Deep Coal Mining

Wenyue Qi,[1,2] **Jixiong Zhang**,[1,2] **Nan Zhou**,[1,2] **Zhongya Wu**,[1,2] **and Jun Zhang**[3]

[1]*State Key Laboratory of Coal Resources and Safe Mining, Xuzhou 221116, China*
[2]*School of Mines, China University of Mining and Technology, Xuzhou 221116, China*
[3]*Shandong Tang Kou Coal Industry Co., Ltd., Jining 272055, China*

Correspondence should be addressed to Wenyue Qi; qwy7604352@163.com and Nan Zhou; zhounanyou@126.com

Received 10 July 2018; Revised 15 October 2018; Accepted 11 November 2018; Published 6 January 2019

Academic Editor: Hassan Haddadpour

Deep coal mining is unavoidable, and the complex mining environments and the increasing dangers associated with ultrahigh energy accumulation and release from mining disturbances renders it extremely difficult to maintain a safe and stable stope. Solid backfilling technology directly uses coal gangue and other solid wastes in the mining area to fill the gob after mining. Support from the backfill body can inhibit the movement of overlying rock strata and significantly alleviate the influence of mining. In this study, the correlations between the deformation of gangue filling material and the characteristics of energy dissipation were examined under lateral uniaxial compression. The strain energy density distributions of backfilling and caving mining methods were simulated using numerical modeling. The results showed that the strain energy density distribution of backfilling mining was less concentrated, and its peak value was lower than that of caving mining by 51.0%, indicating that backfilling could effectively reduce the amount of energy released from mining rocks. The dense backfill mining area of the No. 9301 face in Tangkou Coal Mine was used as a case study. Measures for controlling the backfill body compaction for reducing the amount of energy released from mining rocks were proposed. These measures include optimizing the support structure and filling material formula, controlling the preroof subsidence, and ensuring an appropriate number of tamping strokes. The monitoring results of the backfilling quality, surface subsidence, and microseismic energy of No. 9301 working face in Tangkou Coal Mine showed that when the backfill body filling ratio control value was 82.28%, the total number of microseisms and the amount of energy released from the mining working face were significantly lower compared to those of the caving method. This study demonstrated that the backfill body could effectively reduce the amount of energy released from mining rocks, thereby realizing management of mine earthquake and sustainable deep coal mining.

1. Introduction

With the continuous and high-intensity mining of shallow coal resources and the depletion of coal resources in the eastern region, the resource development in China continues to move toward deep-earth mines at 1000 m to 2000 m. According to the incomplete survey, there are more than 140 deep coal mines, of which 50 have a depth of more than over 1000 m, especially the mining depth of Suncun Coal Mine has exceeded 1500 m. At these depths, the high concentration of stope stress results in the accumulation and release of ultrahigh mining energy. The frequency and intensity of the rockburst also increase significantly. The prevention and control of rock energy in deep coal mining are facing severe challenges [1–5]. Scholars over the world have proposed methods to control the energy accumulation in deep mining. Blake et al. [6] discovered an abnormal increase in microseismic (MS) activity before rock bursts induced by roof fracturing in the process of monitoring test in a hard rock mine. Ortlepp [7] provided strong evidence of an extremely violent fracturing that induced significant rock bursts in the faulting process during stoping of a highly stressed remnant

in a deep gold mine by MS monitoring. Zhang et al. [8] proposed a method for hazard assessment in mines based on seismic energy distribution. Abdul-Wahed et al. [9] set up a close correlation between the location of seismic activity and induced stresses in the ground surface of the working areas by comparing the seismic activity and results of a numerical modeling of an advancing coalface with observations. Chen et al. [10] found that seismic energy and event count steadily increased accompanied by stress increase. Lu et al. [11–13] analyzed the frequency-spectrum evolutionary rule and precursory characteristics by experimental tests for combined coal and rock sample rock burst failure and in situ measurements of a strong rock burst in a coal mine.

As one of the core green mining technologies, solid backfilling mining technology (SBMT) [14–16] directly places coal gangue and other solid wastes into the gob after mining. It is widely applied in resolving many frontier scientific issues in the field of coal mining, such as deep mining [17], no-waste mining [18, 19], safe mining of coal and associated resources [20], and safe hard roof mining [21–23]. Compared with conventional caving mining, the roof of the backfilling stope is only subjected to bending deformation, and the key layer also only undergoes a slight bending deformation from the load of the overlying strata. Therefore, the support from the backfilling body showed a clear controlling effect on reducing the mining influence. However, the research mainly focuses on rock formation and mining pressure of SBMT, in-depth studies on the mechanism by which the backfill body helps reduce the amount of energy released during mining have not been conducted. Therefore, based on a new perspective of energy, this paper mainly studies the evolution of energy during filling material compression and coal seam excavation.

In this study, the correlations between the deformation and acoustic emission (AE) energy dissipation of the gangue filling material were tested under confined compression. The evolvement of mining energy distribution, while using backfilling and caving mining methods, was analyzed by numerical simulation of FLAC^{3D}. Based on the analysis of the energy release results, measures for reducing the amount of energy released from mining rocks by controlling the backfill body compaction were proposed. At the same time, the backfilling quality, surface subsidence, and mining energy between backfill mining working face and caving mining working face were measured, verifying the accuracy of the result. The results showed that backfill body could effectively control the stope energy accumulation and release, which is of great significance for realizing a safe, efficient, and green mining of deep coal resources.

2. Effect of Backfilling on Mining Influence

At the caving roof control working face, the overlying strata supporting system consists of only the coal wall before roof fracture. As the working face advances, the formed cantilever beam structure continues to expand until the suspended area becomes extremely large and causes fractures of the overlying strata. The support system transforms into a composition of "coal wall-hydraulic support-fractured swelling gangue in the collapsed gob" (Figure 1(a)). Then, the roof fractures periodically as the working face advances. The bearing stress and the overlying strata displacement both change significantly, showing an obvious mining influence.

At the backfilling mining working face, the gob is constantly filled by filling materials. Therefore, the overlying strata supporting system always consists of "coal wall-backfilling mining hydraulic support-backfill body" (Figure 1(b)). Supports from the backfill body inhibit the bending and subsidence of the roof, which will not be subjected to periodical fractures. There is no obvious initial and periodic pressure phenomenon. The bearing stress and overlying strata displacement only change slightly. The mining influence is not obvious. The stress concentration coefficient is significantly smaller than that of caving mining. Therefore, backfilling mining can significantly reduce the movement of overlying strata and mining influence.

3. Dissipation Characteristics of Energy in Compressed Gangue

3.1. Experimental Materials. The gangue samples were selected from the excavation gangue of Tangkou Coal Mine in Shandong. The gradations are 0–10 mm, 10–20 mm, 20–30 mm, 30–40 mm, and 40–50 mm, as shown in Figure 2.

3.2. Experimental Equipment. Two sets of devices, namely, the load control system and AE monitoring system, were used for the test. The load control system uses a microcomputer-controlled electrohydraulic servo universal testing machine. The maximum pressure is 1000 kN. The experimental process can be accurately controlled, and the required data can be recorded using a computer program. The sample container is a compacted steel cylinder with a depth of 300 mm, an inner diameter of 250 mm, and a maximum loading height of 270 mm. The AE monitoring system uses the PCI-2 AE testing and analyzing system developed by the Physical Acoustic Corporation (USA). The six evenly placed Nano30 AE sensors at the top and bottom ends of the steel cylinder could automatically count and store the AE parameters and realize real-time monitoring and positioning of the AEs. The experimental equipment is shown in Figure 3.

3.3. Experimental Results

3.3.1. Compaction Properties of Backfill Materials. The compaction deformation curves of gangue samples in different gradation conditions (0–10 mm, 0–20 mm, 0–30 mm, 0–40 mm, and 0–50 mm) are shown in Figure 4.

The entire deformation process of gangue can be divided into three stages: rapid deformation (0–2 MPa), slow deformation (2–10 MPa), and stable deformation (10–22 MPa). In the rapid deformation stage, a small stress could cause a relatively large deformation of the gangue sample. The relative states between particles are unstable, such that the voids close quickly, and the deformation resistance is relatively low. In the slow deformation stage, the large particles

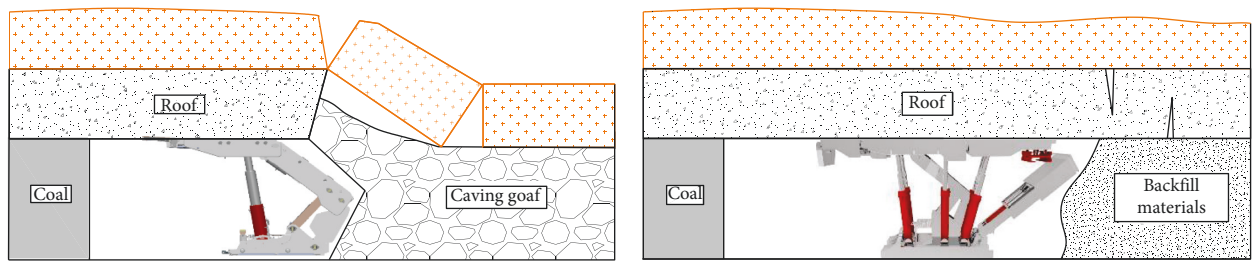

(a) (b)

Figure 1: Surrounding rock-supporting system in caving stope and backfill stope. (a) Caving mining method. (b) Backfilling mining method.

(a) (b) (c) (d) (e)

Figure 2: Gangue samples of different gradations. (a) 0–10 mm, (b) 10–20 mm, (c) 20–30 mm, (d) 30–40 mm, and (e) 40–50 mm.

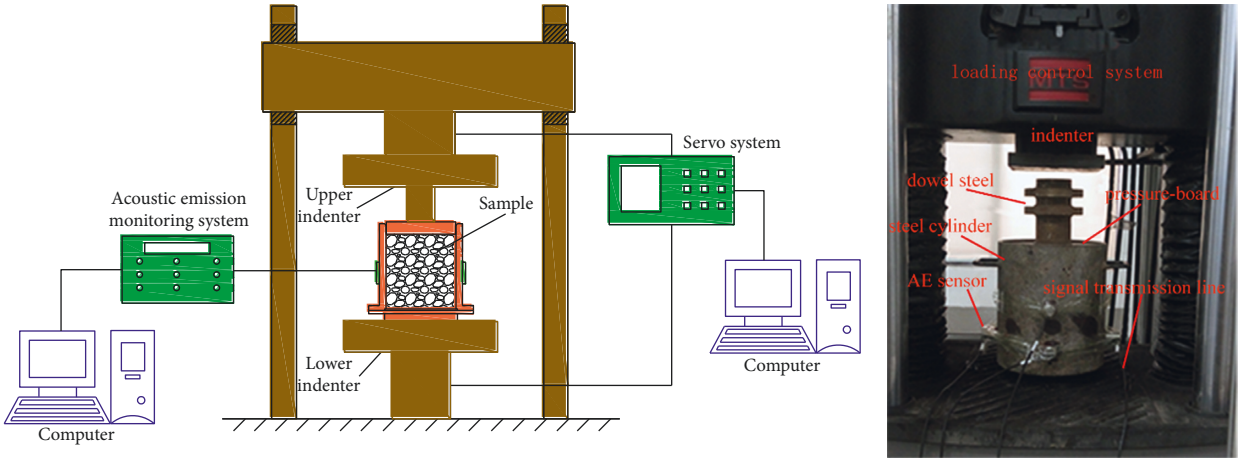

(a) (b)

Figure 3: Experimental equipment.

break into small ones, which then refill the voids, thereby strengthening the deformation resistance of the gangue sample rapidly. In the stable deformation stage, a relatively large stress can only induce a small strain in the gangue sample. The deformation is mainly manifested as the compression of residual voids, the rebreakage of gangue into smaller particles, and the filling of regenerated voids. The deformation resistance of gangue is significantly enhanced in this stage. Under the same compaction stress, the larger the particle size, the larger the strain. This is because there are relatively more voids between large particles, and the strain from void closure is larger than that from particle breakage and deformation. The stress increases exponentially with strain under lateral compression for all the gangue samples. The collected data are fitted to the equation $\sigma = a_1 e^{a_2 \varepsilon} + a_3$.

3.3.2. Dissipation Characteristics of AE Energy in Compressed Gangue. The dissipation characteristics of energy were analyzed by studying the variations in AE energy (E), cumulative counts (ΣN), cumulative energy (ΣE) with strain, and the spatial distribution of AE events at different time nodes. In the particle size range of 0–50 mm, the variations

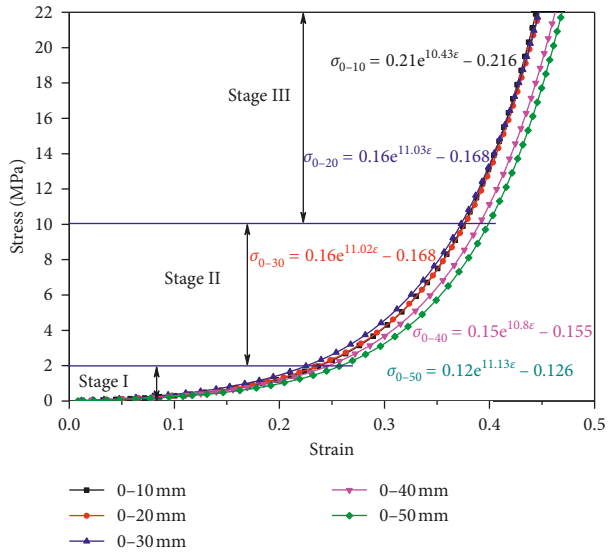

Figure 4: Stress-strain curves for gangue samples of different particle sizes.

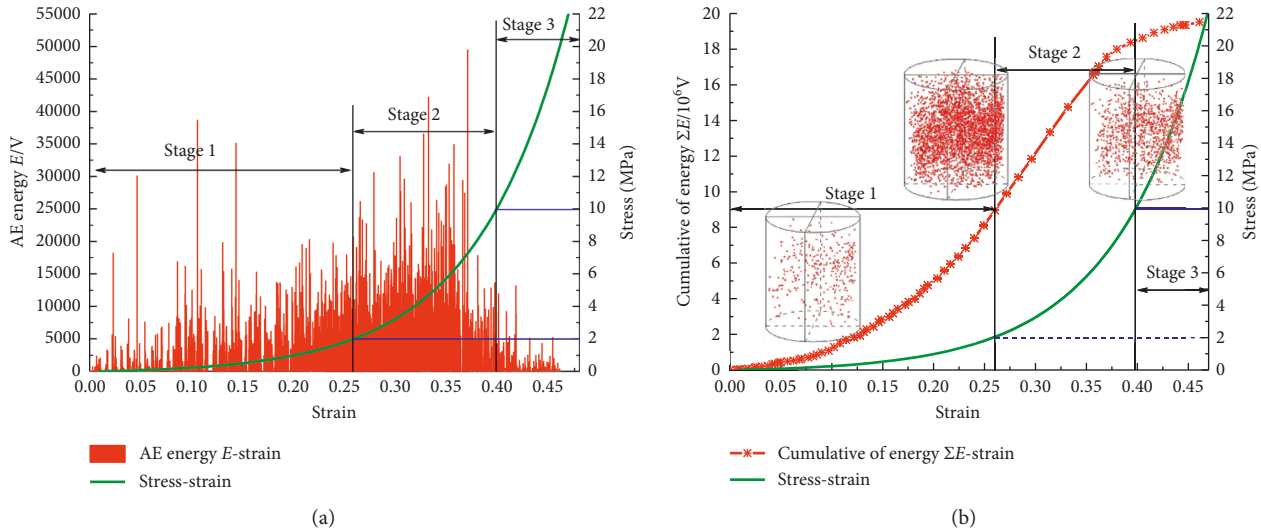

Figure 5: Variations in AE energy and cumulative energy with strain on stress-strain curve. (a) AE energy. (b) Cumulative energy.

in stress, AE energy, cumulative energy with strain, and the spatial distribution of AE events are shown in Figure 5.

The entire AE energy dissipation process can be divided into three stages: slow energy dissipation, accelerated energy dissipation, and attenuated energy dissipation. These stages correspond to rapid deformation, slow deformation, and stable deformation stages in the deformation process, respectively. In the slow energy dissipation stage of AE activities, the AE energy was at a relatively low level. The compaction force mainly worked on rotating and adjusting the gangue particles and closing the voids between them. The AE event locations were scattered within the gangue samples. Most of the events occurred at the contacting points on the edges of the particles, which consumed relatively less energy. As the strain of the gangue samples entered the slow deformation stage, the corresponding AE activities entered the accelerated dissipation stage. More AE signals were recorded, and their spatial distribution became denser. The corresponding hopping signals also increased. The AE event locations gradually spread toward the blank area and became denser. Significantly, more event location points were detected in the center than at the end of the samples, and the energy dissipation rate also increased. This was probably because the compaction force mainly worked on breaking the stable contact structure between gangue particles. The concentrated stress generated at the angular edges of the particles led to their massive breakage. As the strain continued to increase, the AE activities entered the attenuation stage, which corresponds to the stable deformation stage in the stress-strain curve. The particle sizes of gangue samples decreased significantly at this stage, and the dominant AE signal was the friction-induced AE, which was generated as a

result of rubbing and colliding between particles during slippage and overturning. However, the occurrence frequency of hopping signals decreased significantly. Moreover, owing to the low probability of secondary breakage for gangue with small particle size, the AE activities were extremely limited.

4. Temporal and Spatial Distribution Characteristics of Energy Release from Mining Rocks in Backfill Stope

4.1. Simulation Method

4.1.1. Simulation Methods for Strain Energy. By using the equation $\sigma = a_1 e^{a_2 \varepsilon} + a_3$, which is derived by fitting the mechanical property test results of the solid backfill body, the compressive tangent modulus E_g of the backfill body can be obtained by the following equation:

$$E_g = \frac{d\sigma}{d\varepsilon} = \frac{1}{a_1 a_2} e^{\varepsilon / a_1} = \frac{1}{a_1}\sigma + \frac{a_3}{a_1 a_2}. \quad (1)$$

The compressive tangent modulus E_g changes linearly with strain. At a fixed stress value, E_g can be considered as the elastic modulus of the filling material subjected to a constant stress. The bulk modulus K and shear modulus G required for the Mohr–Coulomb model can be calculated. By using the inbuilt FISH language in FLAC^{3D}, the nonlinear compaction procedure is programmed accordingly:

$$\begin{cases} K = \dfrac{E_g}{3(1-2u)}, \\ \\ G = \dfrac{E_g}{2(1+u)}. \end{cases} \quad (2)$$

The strain energy density, which is strain energy per unit volume, in a spatially varying stress state is given by the following equation:

$$v_\varepsilon = \frac{1}{2}\left(\sigma_1 \varepsilon_1 + \sigma_2 \varepsilon_2 + \sigma_3 \varepsilon_3\right). \quad (3)$$

Combined with the generalised form of Hooke's law, the strain energy density in the coal rock mass is obtained as follows:

$$v_\varepsilon = \frac{1}{2E}\left[\sigma_1^2 + \sigma_2^2 + \sigma_3^2 - 2u\left(\sigma_1\sigma_2 + \sigma_2\sigma_3 + \sigma_1\sigma_3\right)\right], \quad (4)$$

where σ_1, σ_2, and σ_3 denote the three principal stresses, while ε_1, ε_2, and ε_3 are the three principal strains. Moreover, E and u represent the elastic modulus and Poisson's ratio of coal rock masses, respectively. The three principal stress values of each point in the coal body ahead of the working face could be calculated through numerical computation. The strain energy density at each point in the coal body could then be obtained.

4.1.2. Model Establishment and Numerical Solution. FLAC^{3D} developed by Itasca Consulting Group, Inc., is widely used in mining engineering; and it is capable of three-dimensional structural force behavior simulation and energy evolution analysis of soil, rock, and other materials. In FLAC^{3D} software, the procedure for strain energy calculation is compiled in FISH [24], in accordance with equation (4), thus giving the distribution of strain energy density in SBMT. A model of 700 m × 270 m × 600 m (length × width × height) was established using the Mohr–Coulomb model according to the engineering-geological conditions of No. 9301 working face of Tangkou Coal Mine (Figure 6). The rock stratum thickness was approximately rounded according to the actual conditions. The physical and mechanical parameters were obtained from laboratory tests (Table S1). Furthermore, the meshes depicting those strata surrounding the coal seams are refined, and the model was divided into 520,800 elements and 543,414 nodes. The boundary conditions were set such that the horizontal freedom was constrained by the walls, whereas the freedom in all three directions was constrained by the bottom, i.e., a fixed bottom. No boundary conditions were applied to the top. Moreover, a compensation stress of 12.5 MPa was applied. In addition, coal columns of 100 m were left at the boundaries to eliminate the influence of boundary conditions on the excavation process. First, the in situ stress fields when applying compensated stress to the top surface and under the self-weight of rock strata were, respectively, simulated, followed by simulation of the excavation and backfill processes. The variations in mining energy were simulated for the backfilling method (filling ratio of 82%) and the caving mining method, recording the strain energy density distribution at the distance from the working surface of 48 m, 72 m, 112 m, and 200 m, respectively.

4.2. Evolution of Strain Energy Density with Advancing Working Face. The distributions of strain energy density of the surrounding rock mass at different advancing distances of the working face using backfilling and caving methods obtained by Surfer are shown in Figures 7 and 8, respectively. An obvious increase in the strain energy density around the stope working face could be observed in the initial mining phase while using the caving method. When the advancing distances of the working face were at 48 m, 72 m, 112 m, and 200 m, the corresponding peak horizontal strain energy densities at the center of the coal seam were 921 kJ/m^3, 1,010 kJ/m^3, 1,096 kJ/m^3, and 1,168 kJ/m^3, respectively, whereas the in situ strain energy density was only approximately 360 kJ/m^3. It can be concluded that the caving mining method could lead to a significant increase in the stope strain energy density. No areas with obviously increased strain energy density formed while using the backfilling method in the initial or subsequent mining phases. Furthermore, no significant changes were observed as the working face advanced. When the advancing distances of the working face were at 48 m, 72 m, 112 m, and 200 m, the corresponding peak strain energy densities were 517 kJ/m^3, 531 kJ/m^3, 549 kJ/m^3, and 573 kJ/m^3, which did not vary significantly. Compared with the caving mining stope, the backfilling mining stope was in an environment with slight energy increase. The overall destruction of the surrounding

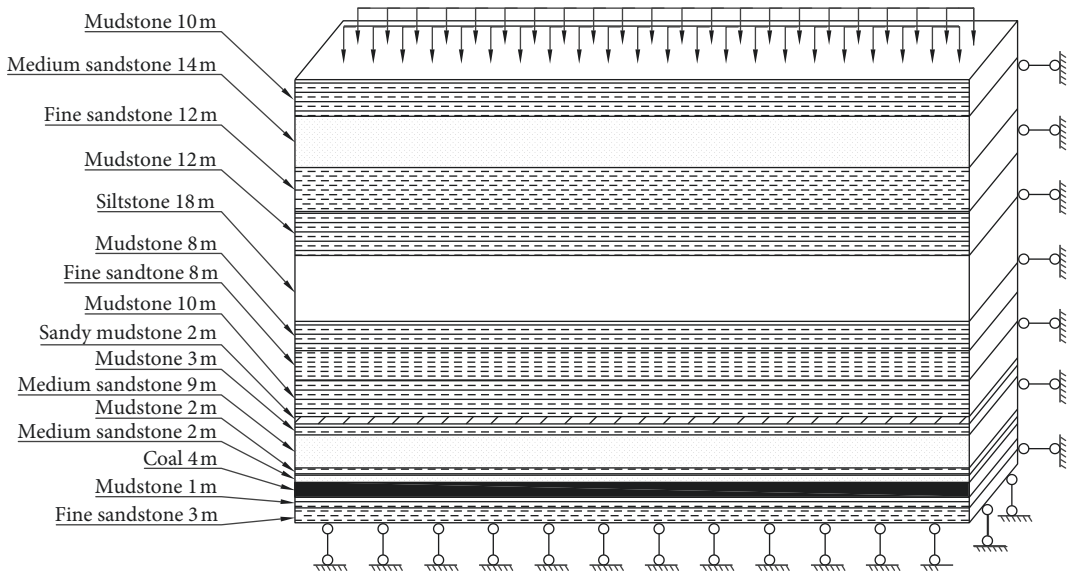

Figure 6: Numerical analysis model and basic parameters.

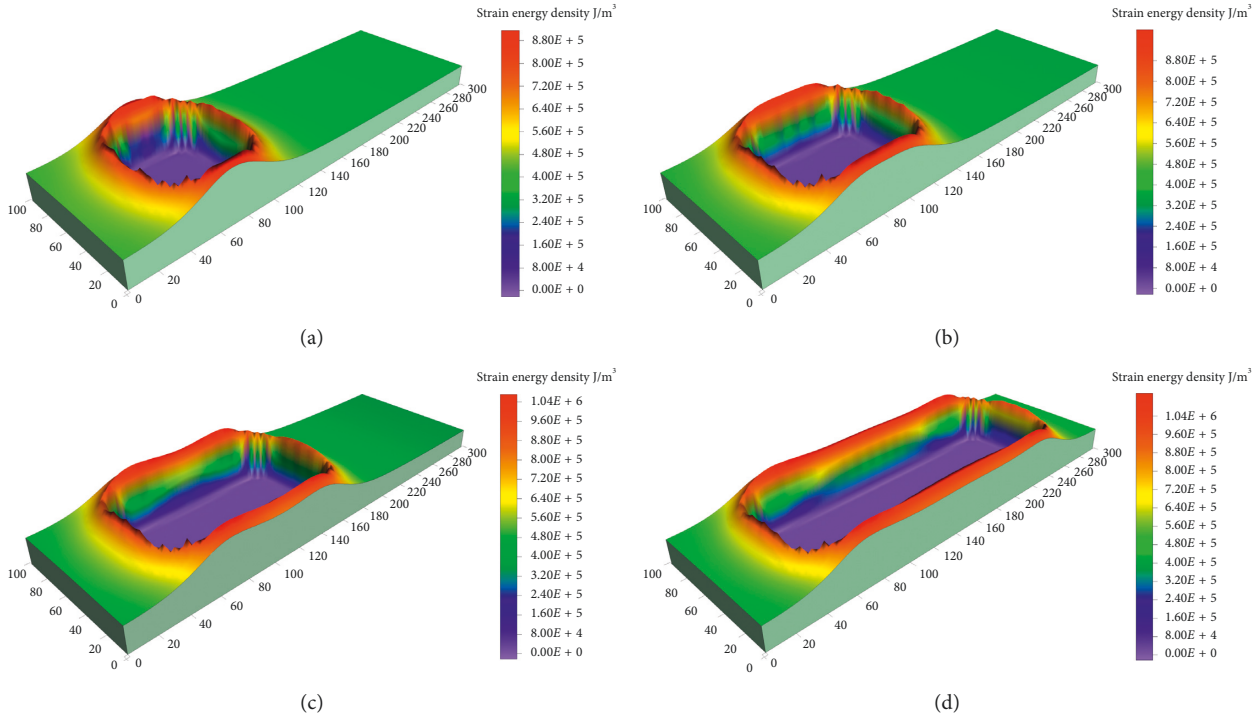

Figure 7: Distribution of strain energy density at different advancing distances when using caving mining method. (a) Working face advanced to 48 m. (b) Working face advanced to 72 m. (c) Working face advanced to 112 m. (d) Working face advanced to 200 m.

rock mass was mitigated, and the amount of energy released was significantly reduced.

The strain energy density distributions at different mining locations in the central axis of the working face can be obtained by examining the cross section along the working face advancing direction, as shown in Figure 9. The following can be observed:

(1) As the working face advanced, the strain energy density in the backfill body increased gradually and reached the maximum when the working face advanced 200 m. The distribution along the working face advancing direction has the shape of an inverted basin, where the strain energy density was high in the middle and low along the side.

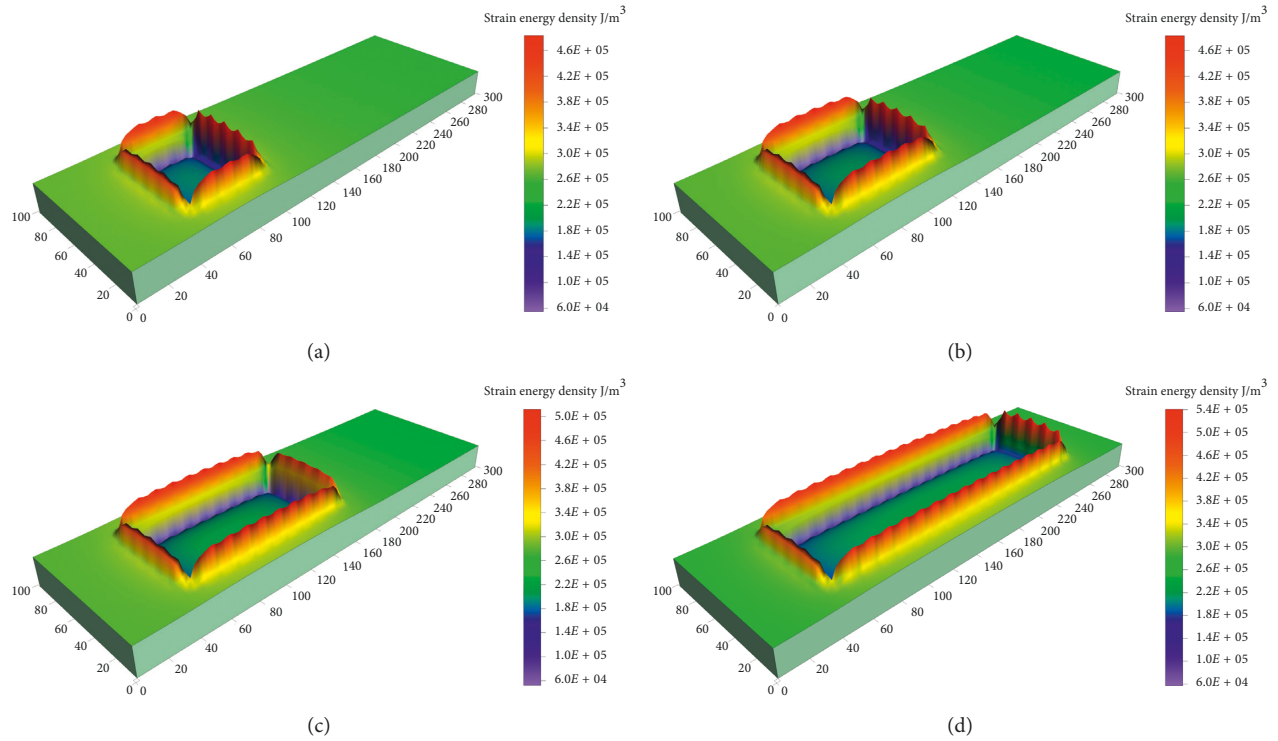

Figure 8: Distribution of strain energy density at different advancing distances when using backfilling mining method. (a) Working face advanced to 48 m. (b) Working face advanced to 72 m. (c) Working face advanced to 112 m. (d) Working face advanced to 200 m.

(2) In the case of caving mining, as the advancement of a workface, the concentration coefficient of strain energy density increased gradually, as shown in Figure 9(a). When the working face advanced to 48 m, 72 m, 112 m, and 200 m, the corresponding concentration coefficients were 2.56, 2.81, 3.04, and 3.24, respectively. A concentration coefficient in the range of 2.5 to 3.5 indicated a high level of energy accumulation and release as well as a drastic change under the caving mining condition, which led to serious destruction of the surrounding rock mass.

(3) In the case of backfilling mining, as the working face advanced, the concentration coefficient of strain energy density did not change significantly, as shown in Figure 9(b). When the working face advanced to 48 m, 72 m, 112 m, and 200 m, the corresponding concentration coefficients were 1.44, 1.48, 1.53, and 1.59, respectively. A concentration coefficient of approximately 1.5 indicated a low level of energy accumulation and release as well as limited changes under the backfilling condition, where the mining gob was compactly filled by the backfill body. Therefore, there was little destruction of the in situ stress field.

(4) The strain energy densities ahead of the working face of caving stope and backfilling stope showed similar distribution patterns, as shown in Figure 9(c). The strain energy density increased rapidly in the beginning and then dropped slowly after reaching the peak. However, compared with the backfilling method, a wider range of strain energy concentration ahead of the working face was observed when using the caving method. The peak value also occurred at a farther location, and the strain energy density concentration coefficient was relatively larger. In the case of caving method, the strain energy was concentrated within a 45 m range ahead of the working face, and a peak strain energy of 1,168 kJ/m^3 was 10 m ahead of the working face. In the case of backfilling method, the strain energy was concentrated within a 20 m range ahead of the working face, and a peak strain energy of 573 kJ/m^3 was 6 m ahead of the working face. The 51% drop in the peak strain energy density indicated that the backfilling method could effectively reduce the amount of energy released from the mining rock.

5. Measurement and Analysis of Tangkou Coal Mine Project

5.1. Project Overview. Mining area 9301 is the first backfill mining area in Tangkou Coal Mine. It spans approximately 0.3–0.9 km from south to north and 1.0–1.3 km from east to west. The mining area covers approximately 0.85 km^2 area with a total coal reserve of 4.067 million tons. All these coal resources are buried under surface buildings. The coal ore is primarily located at the third mining layer with a thickness range from 2.63 to 5.11 m and an average thickness of

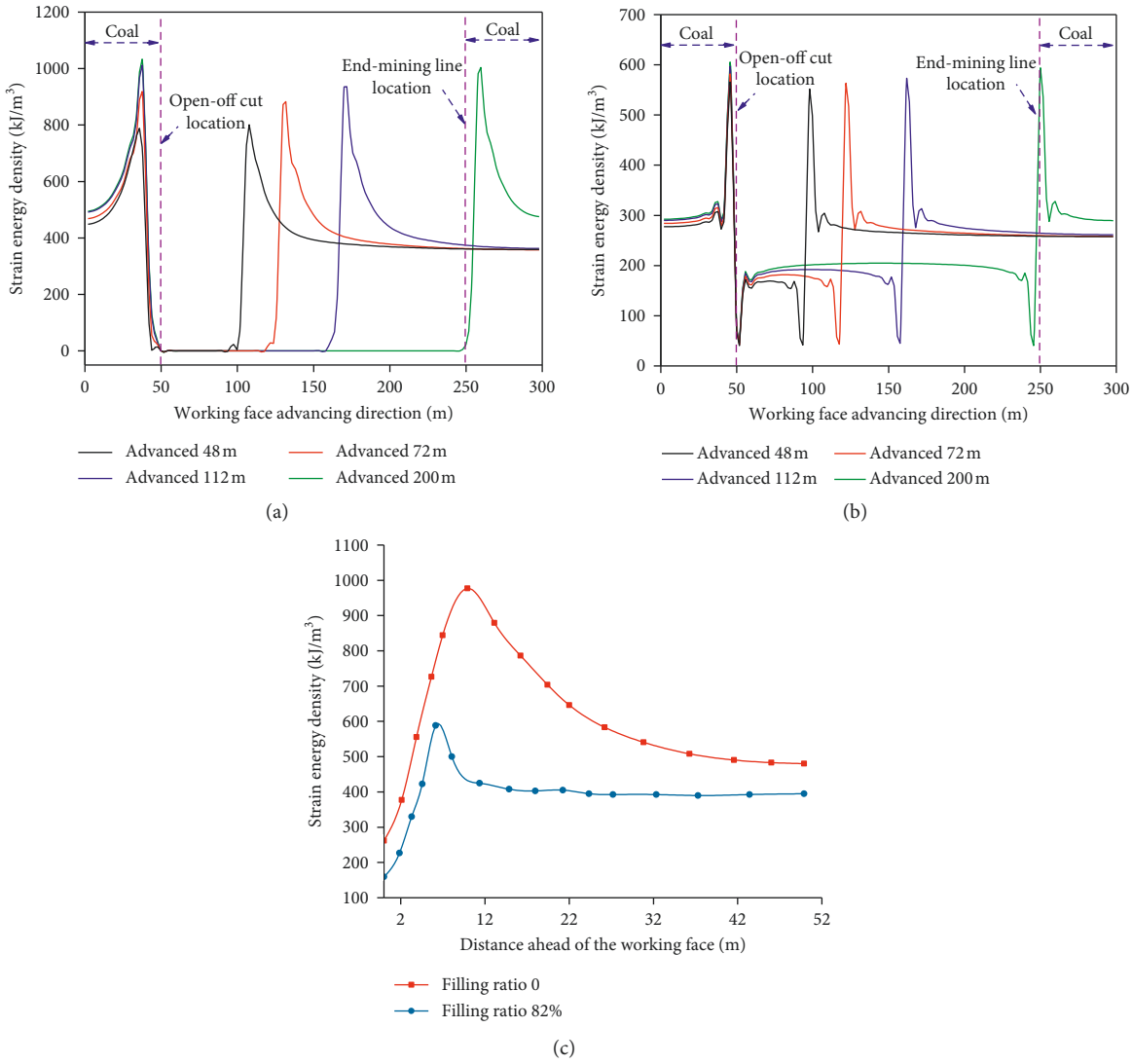

Figure 9: Strain energy density distribution along the central axial direction of working face. (a) Caving method. (b) Backfilling method. (c) Advancing distance of 200 m.

3.50 m. The depth of the coal seam is approximately 1082–1222 m, and the inclination angle of the coal seam ranges from 7° to 16° with an average value of 10°. As assessed by the Beijing Mining Institute of China Coal Research Institute, the burst tendency evaluation results showed a strong rock burst tendency in the coal seam. A total of 9 backfill mining working areas are established in the coal extraction zone with each working area spanning over a length of 60–80 m. A thin coal column of 5 m thickness was kept between adjacent working areas. Figure 10 shows the layout of the mining area and the distribution of underground layers. Because the corresponding surface above the working face was a village, dense filling was set as the controlling criterion for backfill mining.

5.2. Control of Filling Ratio to Weaken Mining Energy. Through numerical analysis, we conclude that the backfill body can effectively reduce amount of the energy released in deep mining. Therefore, guaranteeing the filling ratio is the key factor to the release of mining energy. During the actual solid backfill mining process, the control of the backfill body filling ratio can be performed during the design and implementation stages to achieve a reduction in the amount of energy released [25, 26], as shown in Figure 11. In the design stage, the appropriate tamping force and tamping angle are first determined by optimizing the supporting structure and filling material composition. This ensures a sufficiently high density of the filling material. During the implementation stage, the presubsidence magnitude of top roof, number of tamping strokes, and height of filling material were controlled carefully. More than sufficient filling materials were backfilled in the mining cavity for ensuring a uniform height of the backfill content. The filling ratio was also monitored at different mining locations to obtain instantaneous feedback of the backfill material density. Table 1 shows the main methods of improving roof-controlled backfilling ratio.

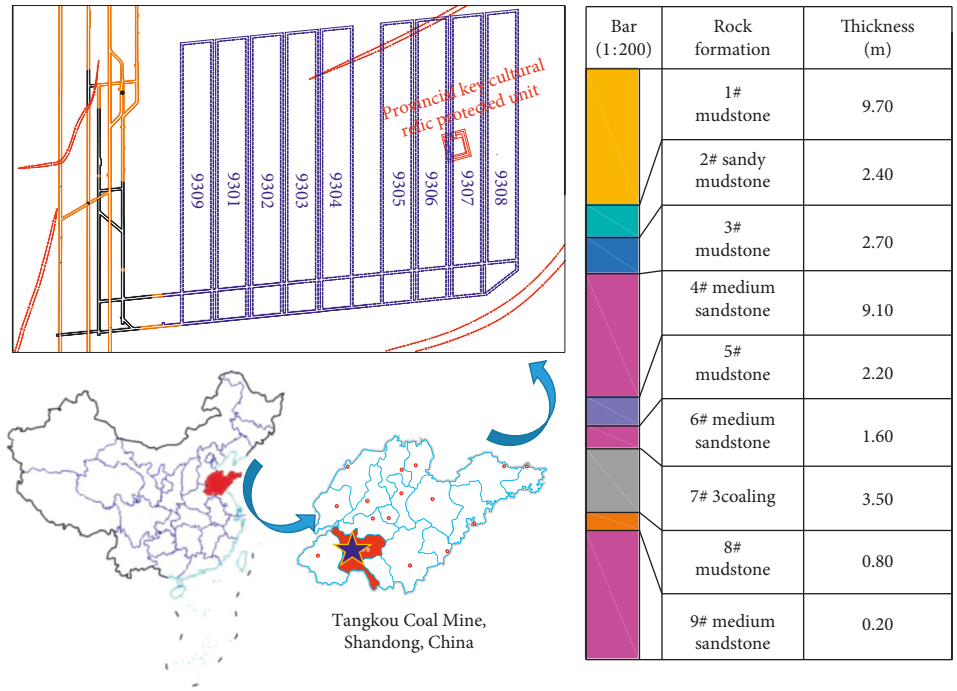

Figure 10: Location of Tangkou Coal Mine and layout of mining area.

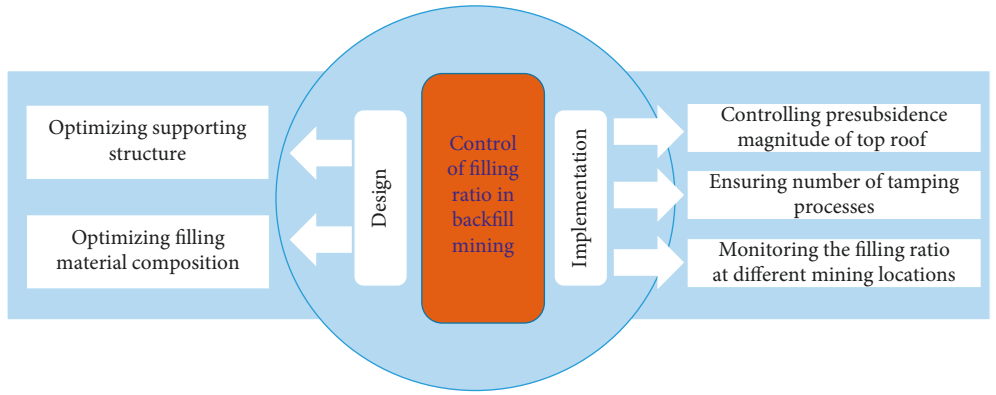

Figure 11: Control method of backfill body density.

5.3. Monitoring of Refilling Mass. A dynamic monitor was installed on the roof inside the filling material for keeping track of the dynamic response of the roof. Specifically, as the refilling process proceeded to different working areas, four roof dynamic monitors were installed as one group as shown in Figure 12(a). The measurement curves are shown in Figures 12(b) and 12(c). The following characteristics were observed from the curves:

(1) The subsidence curve of the roof changes continuously without any sudden jump. This indicates that the roof used for monitoring did not break or slide off during the sampling period. An intense activity of the roof was observed during the early stage of the refilling process. As the refilling proceeds to 188 m, a stable response was observed from the roof. The maximum subsidence of the roof was found to be 620 mm at the peak point. This suggests that the actual filling ratio was controlled at 82.28%.

(2) With increasing subsidence of the roof in the refilling area, the refilling stress increased as the refilling materials were tamped gradually. The internal stress of the filling material reached a stable value of 22.4 MPa when the working plane reached 89 m. This value approaches the original rock stress, which indicates that the bending deformation of the overlying stratum was equilibrated by the support from the refilling material.

5.4. Measurement of Microseismic Energy. During the mining of No. 9301 working face, the MS energy was measured using an MS monitoring system. The recorded results were compared with the No. 1303 fully mechanized mining face located approximately 1,000 m to its north. Both working faces had similar burial depths and dip angles. The measured energy distributions of microseismicity are shown in Figure 13, and the MS events are presented in Table 2.

Table 1: Main methods of improving roof-controlled backfilling ratio.

Key parameter	Influencing factor	Corresponding measures
Optimization of the support structure	Equipment performance	Increase the support strength and setting load. Design the hydraulic support ZZC10000/20/40 for solid backfill coal mining with a support strength of 0.82 MPa and a setting load of 8,322 kN Optimize the support structure. Shorten the top beam length of the hydraulic support to 8,045 mm to reduce the distance of face roof under control Design a full-seam tamping mechanism to achieve full-height compaction and increase the tamping capacity to 2 MPa
Optimization of filling material formula	Mechanical properties Filling material properties	Adjust the sieving and crushing settings to crush the gangues down to sizes of 50 mm or lower to reduce the backfill body compression ratio Add water during transportation to optimize the moisture content of the solid filling materials, improve the material adhesiveness, and minimize the natural rest angle
Preroof subsidence	Roof conditions Backfilling technique	Install two layers of metal mesh in cases of false roof or broken roof Parallel operations of mining and backfilling to reduce the time and span of unsupported roof before filling Using hydraulic roof support to ensure prompt support and reduce roof deformation
Tamping strokes	Backfilling technique	Ensure that the tamping counts for each backfilling are more than 10 strokes Improve the initial loaded stress on the backfill body and reduce the compression ratio Determine the initiation of the next cycle of coal extraction by the backfilling quality
Dynamic monitoring of the filling ratio	Monitoring system	Install equipment for monitoring support resistance, tamping force, and filling ratio to achieve real-time filling quality monitoring Establish a step-by-step inspection system to check and rectify the filling quality
Common measures	Operating specification	Establish complete training and assessment specifications and improve the technical capabilities of backfilling operators Form a five-people team to perform backfilling alternatively and minimize the influence of personal reasons on the filling quality Adjust salary based on filling quality to motivate operators

Six MS events with energy greater than 5,000 J were detected from the No. 9301 backfill mining working face, whereas 49 such events were detected from the No. 1303 fully mechanized mining face. Among them, seven events had energy greater than 10,000 J, and the maximum MS energy reached 17,100 J. The total number of MS events and average MS energy measured from the No. 9301 working face were much smaller compared with the ones from the No. 1303 working face. No large energy release was detected from the No. 9301 working face, indicating that the solid backfilling mining method effectively reduced the amount of energy released.

5.5. Measurement of Surface Subsidence. In order to monitor the effect of underbuilding refilling mining on the surface buildings at mining area No. 930, a monitor system was designed with a monitor point spacing of 25 m and a control point spacing of 50 m, based on the actual condition at the ground surface. Figure 14 shows the detailed installation map of surface subsidence measuring points and the monitoring results. Until now, the coal extraction activities at working areas No. 9301, No. 9302, and No. 9303 are already finished, and no significant deformation was observed on any surface buildings. The maximum surface subsidence was far smaller than the critical deformation value required for inducing permanent damage to the masonry buildings. Hence, these measurement results demonstrate that a filling ratio of 82.28% can effectively protect the surface buildings from mining activity .

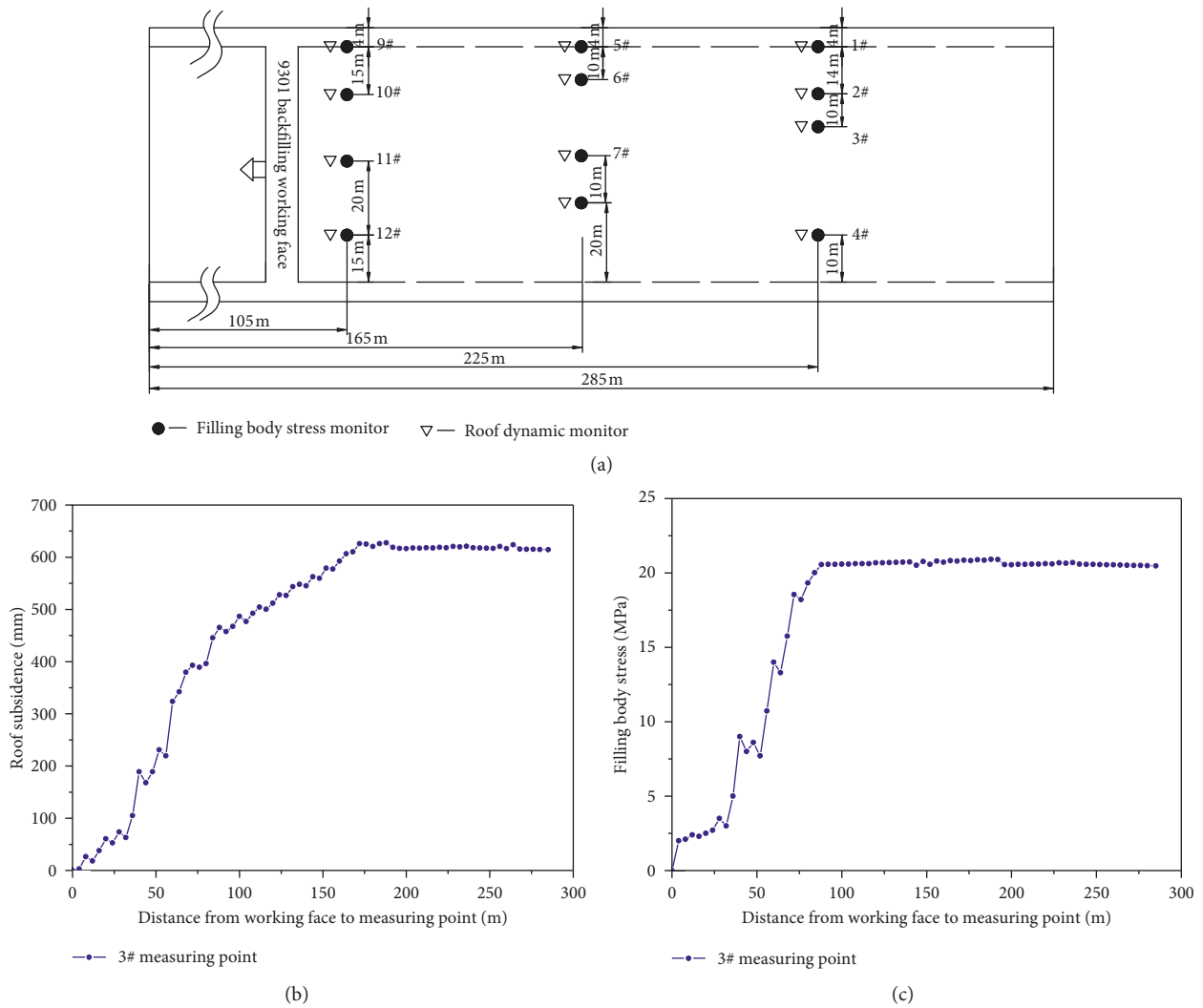

Figure 12: Roof dynamic subsidence measurement. (a) Actual measurement plan. (b) Roof subsidence curve. (c) Stress-strain of filling material.

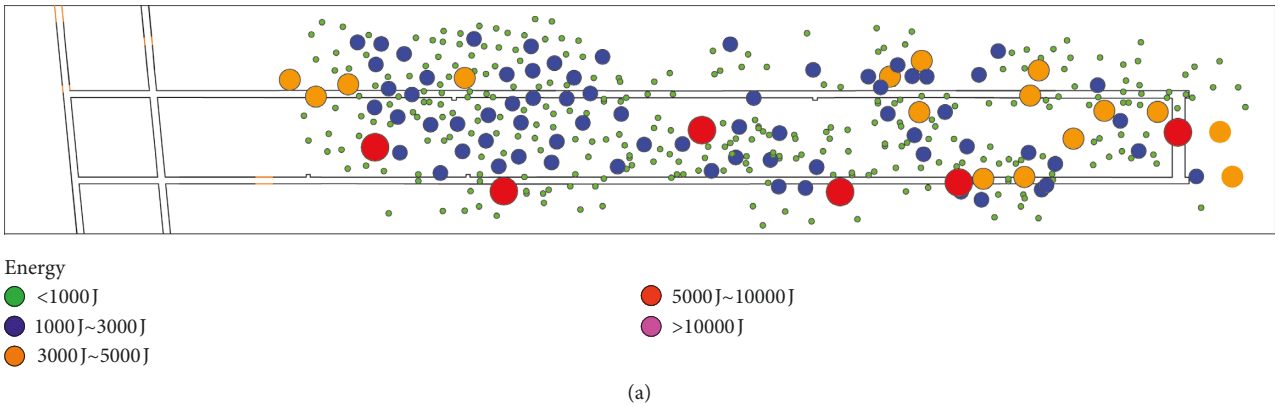

Figure 13: Continued.

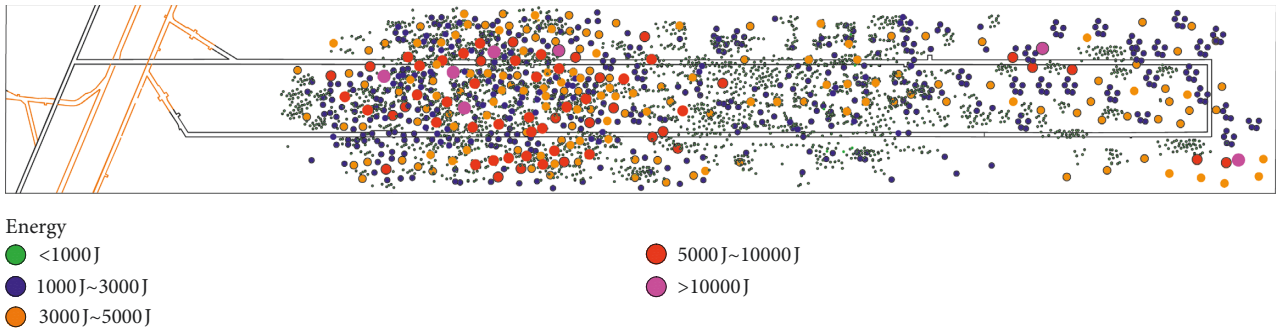

(b)

Figure 13: Energy distribution of microseismicity during mining. (a) No. 9301 backfill mining working face. (b) No. 1303 caving mining working face.

Table 2: Statistics of microshock during extraction of 9301 and 1303 workface

Energy range	Number of microseismic events from No. 9301 backfill mining working face	Number of microseismic events from No. 1303 fully mechanized mining face
<1,000 J	143	743
1,000–3,000 J	60	349
3,000–5,000 J	16	165
5,000–10,000 J	6	42
>10,000 J	0	7
Total number of microseismic events	225	1,307
Maximum microseismic energy (J)	6,400	17,100
Average microseismic energy (J)	858	1,260

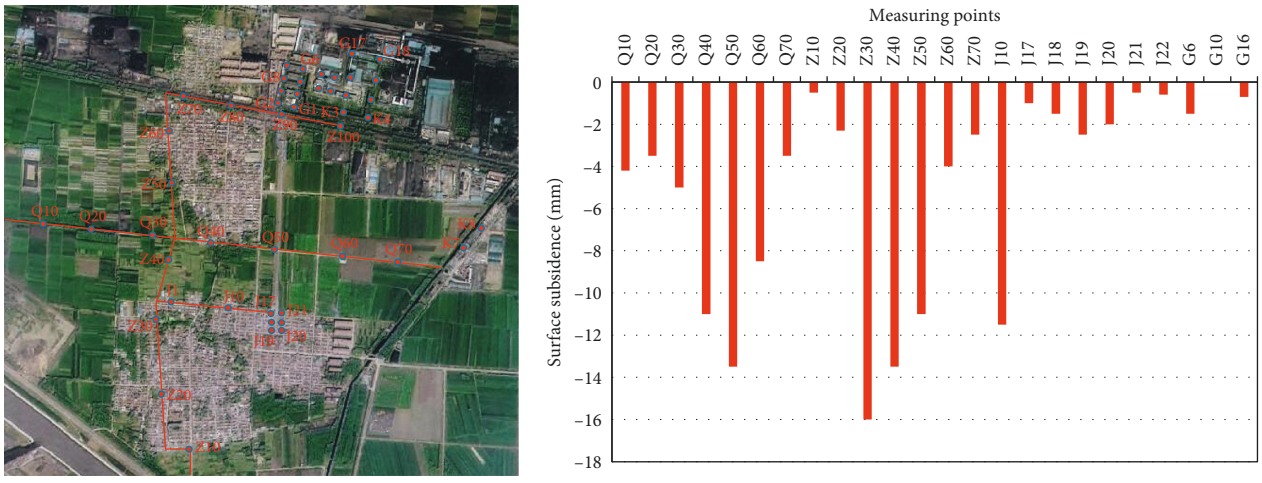

(a) (b)

Figure 14: Surface subsidence monitoring results at the working area. (a) Actual measurement plan. (b) Surface subsidence measured from the measuring points.

6. Conclusions

(1) In the compaction process of the gangue samples, the AE energy evolution corresponded well with the stress-strain curves. During the three deformation stages, namely, rapid deformation, slow deformation, and stable deformation, shown in the stress-strain curves, the monitored AE activities showed three corresponding energy dissipation stages, i.e., slow dissipation, accelerated dissipation, and attenuated dissipation. The locations of detected AE events showed the most AE activities at the edge of the gangue sample center. The compression test of gangue samples provided data to support the numerical calculations of energy distributions in the mining stope.

(2) Based on the principle of low degree of disturbance and destruction of rock mass and lack of mining pressure appearance at the backfill mining stope, the mechanism by which the backfill body reduces the amount of energy released during mining of rocks was proposed. The evolving characteristics of strain energy density with the advancing working face were revealed. Compared with the caving mining stope, the backfilling mining stope had a relatively less concentrated strain energy density distribution, and the peak value was 51% less. This indicated that the backfilling method effectively reduced the amount of energy released from the mining rocks.

(3) Based on the mining geological conditions of No. 9301 solid backfilling mining working face in Tangkou Coal Mine, measures for reducing the amount of energy released by controlling the compaction of filling materials were proposed. These measures include optimization of the support structure and filling material formula, controlling the preroof subsidence, ensuring an optimal number of tamping strokes, and dynamic monitoring of the filling ratio. Engineering practices showed that a filling ratio control value of 82.28% could effectively reduce the amount of energy released, thereby realizing safe and sustainable deep coal mining.

Data Availability

The data used to support the findings of this study are included within the article.

Conflicts of Interest

The authors declare that there are no conflicts of interest regarding the publication of this article.

Authors' Contributions

Wenyue Qi and Nan Zhou contributed equally to the work and should be regarded as co-first authors.

Acknowledgments

The authors gratefully acknowledge the financial support for this work, provided by Project 51874287, which is supported by the National Natural Science Foundation of China. This work was supported by the National Science Fund for Distinguished Young Scholars (51725403).

Supplementary Materials

Figure S1: the distribution of z-direction stress at different advancing distances when using caving mining. Figure S2: the distribution of z-direction stress at different advancing distances when using backfilling mining. Table S1: the physical and mechanical parameters of rock formations in the numerical model. (*Supplementary Materials*)

References

[1] H. Xie, G. Feng, J. U. Yang, and S. University, "Research and development of rock mechanics in deep ground engineering," *Chinese Journal of Rock Mechanics and Engineering*, vol. 11, pp. 2161–2178, 2015.

[2] H. P. Xie, F. Gao, Y. Ju, M. Z. Gao, R. Zhang, and Y. N. Gao, "Quantitative definition and investigation of deep mining," *Journal of China Coal Society*, vol. 40, no. 1, pp. 1–10, 2015.

[3] H. P. Xie, H. W. Zhou, D. J. Xue, H. W. Wang, R. Zhang, and F. Gao, "Research and consideration on deep coal mining and critical mining depth," *Journal of China Coal Society*, vol. 37, no. 37, pp. 535–542, 2012.

[4] L. Yuan, "Thoughts and suggestions on cracking major scientific and technological problems in deep coal mining," *Science and Technology Review*, vol. 34, no. 2, p. 1, 2016.

[5] C. Hou and S. O. Mines, "Key technologies for surrounding rock control in deep roadway," *Journal of China University of Mining and Technology*, vol. 46, no. 5, pp. 970–978, 2017.

[6] W. Blake, F. Leighton, and W. I. Duvall, "Microseismic techniques for monitoring the behavior of rock structures," Technical Report Archive and Image Library, 1974.

[7] W. D. Ortlepp, "Observation of mining-induced faults in an intact rock mass at depth," *International Journal of Rock Mechanics and Mining Sciences*, vol. 37, no. 1, pp. 423–436, 2000.

[8] M. Zhang, H. Shimada, T. Sasaoka, K. Matsui, and L. Dou, "Seismic energy distribution and hazard assessment in underground coal mines using statistical energy analysis," *International Journal of Rock Mechanics and Mining Sciences*, vol. 64, no. 64, pp. 192–200, 2013.

[9] M. K. Abdul-Wahed, M. Al Heib, and G. Senfaute, "Mining-induced seismicity: seismic measurement using multiplet approach and numerical modeling," *International Journal of Coal Geology*, vol. 66, no. 1, pp. 137–147, 2006.

[10] X. Chen, W. Li, and X. Yan, "Analysis on rock burst danger when fully-mechanized caving coal face passed fault with deep mining," *Safety Science*, vol. 50, no. 4, pp. 645–648, 2012.

[11] C.-P. Lu, G.-J. Liu, Y. Liu, N. Zhang, J.-H. Xue, and L. Zhang, "Microseismic multi-parameter characteristics of rockburst hazard induced by hard roof fall and high stress concentration," *International Journal of Rock Mechanics and Mining Sciences*, vol. 76, pp. 18–32, 2015.

[12] C.-P. Lu, L.-M. Dou, N. Zhang et al., "Microseismic frequency-spectrum evolutionary rule of rockburst triggered by roof fall," *International Journal of Rock Mechanics and Mining Sciences*, vol. 64, no. 6, pp. 6–16, 2013.

[13] C.-P. Lu, L.-M. Dou, X.-R. Wu, and Y.-S. Xie, "Case study of blast-induced shock wave propagation in coal and rock," *International Journal of Rock Mechanics and Mining Sciences*, vol. 47, no. 6, pp. 1046–1054, 2010.

[14] J. Zhang, "Study on strata movement controlling by raw waste backfilling with fully-mechanized coal winning technology and its engineering applications," Doctoral dissertation, China University of Mining and Technology, Xuzhou, China, 2008.

[15] X. X. Miao and J. X. Zhang, "Analysis of strata behavior in the process of coal mining by gangue backfilling," *Journal of Mining and Safety Engineering*, no. 4, pp. 379–382, 2007.

[16] X. Miao, J. U. Feng, Y. Huang, and G. Guo, "New development and prospect of backfilling mining theory and technology," *Journal of China University of Mining and Technology*, vol. 44, no. 3, pp. 391–399, 2015.

[17] J. Zhang, Q. Zhang, F. Ju, N. Zhou, M. Li, and Q. Sun, "Theory and technique of greening mining integrating mining, separating and backfilling in deep coal resources," *Journal of China Coal Society*, vol. 43, no. 2, pp. 377–389, 2018.

[18] J. Zhang, Q. Zhang, Y. Huang, J. Liu, N. Zhou, and D. Zan, "Strata movement controlling effect of waste and fly ash backfillings in fully mechanized coal mining with backfilling face," *Mining Science and Technology*, vol. 21, no. 5, pp. 721–726, 2011.

[19] Z. Qiang, J. Zhang, T. Yang, H. Jia, L. I. Meng, and S. O. Mines, "Study of factors influencing the gap between backfill hydraulic support and roof," *Journal of China University of Mining and Technology*, vol. 43, no. 5, pp. 757–764, 2014.

[20] J. Zhang, Q. Zhang, A. J. S. Spearing, X. Miao, S. Guo, and Q. Sun, "Green coal mining technique integrating mining-dressing-gas draining-backfilling-mining," *International Journal of Mining Science and Technology*, vol. 27, no. 1, pp. 17–27, 2017.

[21] N. Zhou, J. Zhang, H. Yan, and M. Li, "Deformation behavior of hard roofs in solid backfill coal mining using physical models," *Energies*, vol. 10, no. 4, p. 557, 2017.

[22] J. Zhang, B. Li, N. Zhou, and Q. Zhang, "Application of solid backfilling to reduce hard-roof caving and longwall coal face burst potential," *International Journal of Rock Mechanics and Mining Sciences*, vol. 88, pp. 197–205, 2016.

[23] M. Li, N. Zhou, J. Zhang, and Z. Liu, "Numerical modelling of mechanical behavior of coal mining hard roofs in different backfill ratios: a case study," *Energies*, vol. 10, 2017.

[24] Itasca, *Fast Lagrangian Analysis of Continua in 3 Dimension; Version 3.1: User's Guide*, Itasca, Minneapolis, MN, USA, 2007.

[25] N. Zhou, "Mechanism of preventing dynamic hazards under hard roof by solid backfilling technology," Doctoral dissertation, China University of Mining and Technology, Xuzhou, China, 2014.

[26] Q. Zhang, *Roof control mechanism by coordination with backfilled body and backfill support in solid backfill mining technology*, Doctoral dissertation, China University of Mining and Technology, Xuzhou, China, 2015.